Solid-State ^{13}C NMR Analyses for the Structure and Molecular Motion in the α Relaxation Temperature Region for Metallocene-Catalyzed Linear Low-Density Polyethylene

Kazuhiro Kuwabara, Hironori Kaji, and Fumitaka Horii*

Institute for Chemical Research, Kyoto University Uji, Kyoto 611-0011, Japan

Received July 29, 1999

ABSTRACT: The structure and molecular motion of metallocene-catalyzed linear low-density polyethylenes (MLLDPE) have been investigated in the α relaxation temperature region by solid-state ^{13}C NMR spectroscopy. Fully relaxed dipolar decoupling (DD)/MAS ^{13}C NMR spectra are well resolved into the crystalline, crystalline−amorphous interfacial, and rubbery amorphous components at different temperatures above room temperature. Prominent broadening of the crystalline resonance line in the DD/MAS spectra is observed above 60 °C, while the chemical shift anisotropy (CSA) spectra stay almost unchanged from the line shape in the rigid state. This fact indicates, in good accord with the previous results, that the 180° flip motion around the molecular chain axis occurs above 60 °C in the crystalline region with the rate of about 10^5 Hz. Moreover, the segmental exchange between the crystalline and noncrystalline regions, which will be closely associated with the multistep forward and backward 180° flip motions, is clearly confirmed for MLLDPE with butyl branches at 80 °C by 2D ^{13}C exchange NMR spectroscopy. A simple one-dimensional random walk simulation is also performed to elucidate the chain diffusion process that allows the exchange of the crystalline and noncrystalline segments. A T_{1C} analysis for the crystalline component transferred within 1 s by the chain diffusion from the noncrystalline region is further made by a newly developed pulse sequence.

Introduction

In our previous paper,[1] the crystalline−noncrystalline structure for the metallocene-catalyzed linear low-density polyethylene sample (MLLDPE), which was isothermally crystallized from the melt, was characterized in detail by high-resolution solid-state ^{13}C NMR spectroscopy. This sample seems useful for detailed analyses of the structure and molecular motion in the α relaxation temperature region, because the morphological structure is comparatively simple and no significant morphological change occurs by annealing during solid-state ^{13}C NMR measurements.

It is well-known that the dynamic mechanical analysis of polyethylene prior to melting reveals at least three mechanical relaxations, designated as α, β, and γ in the order of decreasing temperature.[2] Although some detailed assignments are still open to debate, the origins of the three relaxations are almost clear. The mechanical α relaxation consists of at least three subrelaxations, namely α_1, α_2, and α_3 in the order of increasing temperature.[3] The α_1 relaxation arises from the interlamellar slip[4] or the deformation of intermosaic regions within the crystalline lamellae.[5] The α_2 relaxation is believed to originate from the thermal oscillation of intracrystalline polymer chains,[3−5] including 180° flip motion about the molecular chain axis as well as the translational motion along the chain axis.[6,7] The reality of the α_3 relaxation is suggested to relate the transition from the orthorhombic to the hexagonal phase.[8,9]

Solid-state ^{13}C NMR spectroscopy is very powerful in investigating the molecular motion and phase structure for solid polymers.[10] When polyethylene samples are measured in the α relaxation temperature region, the spectra mainly reflect the α_2 relaxation. For example, "chain diffusion" was observed by the ^{13}C spin exchange experiments,[11] two-dimensional ^{13}C exchange NMR,[12] and ^{13}C spin−lattice relaxation measurements.[13] The 180° flip motion around the molecular chain axis was also directly observed by ^{13}C dipolar NMR measurements.[14] Veeman et al. found an increase in the half-width of the crystalline resonance line with the increase of temperature in the α relaxation temperature region.[15] They suggested that such motional broadening, reflecting the molecular motion with a rate in the kilohertz domain,[16−18] may be ascribed to the 180° flip motion around the molecular chain axis. However, they did not confirm the mode of the molecular motion with the experimental data using the same samples. One of the purposes of this work is to clarify the mode of the molecular motion in the α_2 relaxation process for MLLDPE with butyl branches. A similar solid-state ^{13}C NMR analysis has been also performed to elucidate the α_3 relaxation for constrained ultradrawn polyethylene fibers.[19]

Previous studies described above on the α_2 relaxation were mainly based on the simple two-phase model where the polyethylene samples consist of only the crystalline and noncrystalline components. However, the noncrystalline component around room temperature contains the crystalline−amorphous interfacial component in addition to the rubbery amorphous component.[1,20−24] The crystalline region seems to be also composed of plural components with different ^{13}C spin−lattice relaxation time (T_{1C}) values,[1,21−23] though the effect of the chain diffusion should be well evaluated in these cases. Solid-state ^{13}C NMR spectroscopy is a useful technique for the separate characterization of the molecular motion for different crystalline and noncrystalline components. In this paper, we also characterize the molecular motions of the crystalline and noncrystalline components in the α relaxation temperature region.

Experimental Section

Samples. Two sorts of LLDPE samples with similar primary structure were used for solid-state ^{13}C NMR measure-

10.1021/ma9912608 CCC: $19.00
Published on Web 05/24/2000

Table 1. Characteristics of Nascent LLDPE Samples

	MLLDPE[a]	MLLDPE12[b]
branch content (per 1000 C atoms)[c]	9.6	9.8
M_n	4.27×10^4	3.69×10^4
M_w	9.65×10^4	9.45×10^4
M_w/M_n	2.3	2.6

[a] From Neste Oy Chemicals. See ref 1. [b] From Japan Polyolefins Co. Ltd. [c] Solution-state ^{13}C NMR.

ments. Both were synthesized with 1-hexene as a comonomer by metallocene catalysis. One sample was pilot-plant resins from Neste Oy Chemicals, which had a weight-average molecular weight (M_w) of 96 500, number-average molecular weight (M_n) of 42 700, and a butyl branch content of ~1.0 per 100 carbons.[1,24] The crystallization was done at 110 °C for 18 h from the melt; this sample is abbreviated as MLLDPE hereafter as done previously.[1] Since the sample amount of MLLDPE is not enough, another LLDPE sample, provided by Japan Polyolefins Co. Ltd., was used for two-dimensional ^{13}C NMR measurements; M_w, M_n, and the butyl branch content are 94 500, 36 900, and ~1.0/100, respectively. This sample was crystallized by slowly cooling from the melt, and it is abbreviated as MLLDPE12 in this work. Characteristics of the two LLDPE samples are listed in Table 1.

Solid-State ^{13}C NMR. Solid-state ^{13}C NMR spectra for MLLDPE were obtained on a JEOL JNM-GSX200 spectrometer operating under a static magnetic field of 4.7 T. The sample was packed into a 7 mm diameter zirconia MAS rotor. ^1H and ^{13}C radio-frequency fields $\gamma B_1/2\pi$ were 62.5−64.1 kHz. The contact time for the cross-polarization (CP) process was 1.0 ms throughout this work. The MAS rate was set to 3 kHz to avoid the overlapping of spinning sidebands on other resonance lines. ^{13}C chemical shift anisotropy (CSA) spectra for the crystalline component were obtained at different temperatures by the CPT1 pulse sequence[25] without MAS. ^{13}C chemical shifts were expressed as values relative to tetramethylsilane (Me_4Si) by using the CH_3 line at 17.36 ppm of hexamethylbenzene crystals as an external reference. Temperature calibration was done by the ethylene glycol method modified for NMR measurements under MAS.[26−28]

Two-dimensional ^{13}C NMR and its related NMR measurements were carried out by a Chemagnetics CMX-400 spectrometer operating under a static magnetic field of 9.4 T. The MAS rate was set to 4 kHz. Other experimental conditions were almost the same as those for the JEOL JNM-GSX200 system.

Results and Discussion

Crystalline−Noncrystalline Structure of MLLDPE at Different Temperatures. Figure 1 shows fully relaxed dipolar decoupling (DD)/MAS ^{13}C NMR spectra of MLLDPE measured at different temperatures above room temperature. Small resonance lines indicated by "b" are ascribed to the butyl branch carbons.[1] Broken lines indicate the respective components for the CH_2 resonance lines basically obtained by using the line shape analysis previously reported.[1,21] Each line at each temperature is found to be well resolved into the crystalline, crystalline−amorphous interfacial, and rubbery amorphous components. Here, the separation of the noncrystalline component into the interfacial and rubbery components was made by using the difference in ^{13}C spin−spin relaxation time (T_{2C}).[1,21] The crystalline component appearing at 32.89 ppm has also been found to consist of three components with different T_{1C} values at each temperature, in accord with the cases for different polyethylene samples reported previously.[1,21−23] We also tried to analyze the T_{1C} relaxation process of this sample in terms of the one-dimensional chain diffusion equation previously proposed.[13] However, the relaxation curve was found not to be well described by

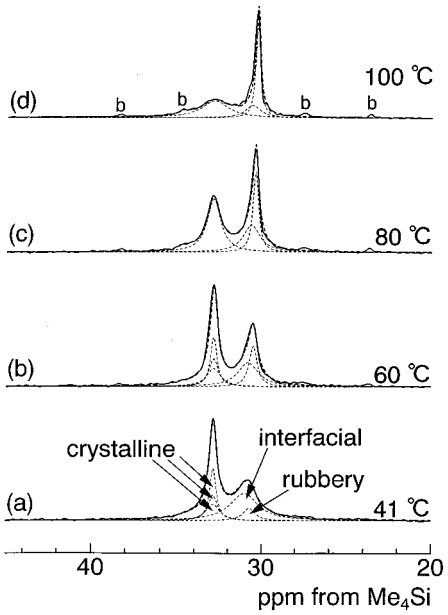

Figure 1. Fully relaxed DD/MAS ^{13}C NMR spectra for MLLDPE at different temperatures. The character "b" indicates the resonance line ascribed to butyl branches.

this equation, suggesting the real existence of plural components with different molecular mobilities. In this paper, therefore, the crystalline component is simply further resolved into three components on the basis of the T_{1C} measurements. To this end, their line shapes are determined in the following way. For convenience, these components are called as the rigid crystalline, less mobile crystalline, and mobile crystalline components in the order of decreasing T_{1C} values.

First, real resonance lines for the three components were obtained by using the differences in T_{1C}. The spectrum of the rigid crystalline component was selectively measured using the CPT1 pulse sequence[25] by setting the T_{1C} decay time τ to 150 s, which corresponds to the value larger than $5T_{1C}$ for the less mobile crystalline component. Next, the spectrum of the less mobile crystalline component was obtained by subtracting the rigid crystalline spectrum from the spectrum measured with the CPT1 pulse sequence by setting $\tau =$ 10 s. In these spectra, the mobile crystalline component completely disappeared due to the short T_{1C} value. As for the mobile crystalline component, the spectrum was obtained by subtracting the rigid crystalline and less mobile crystalline components from the spectrum measured with the CPT1 pulse sequence by setting $\tau = 0.4$ s. These three resonance lines thus obtained were found to be well described by Lorentzian curves with the same chemical shift value and evidently different line widths. Therefore, the least-squares method was carried out for the spectra shown in Figure 1 by using the three Lorentzians for the crystalline component in addition to two Lorentzians[1,21] for the interfacial and amorphous components.

In Table 2, chemical shift values, half-widths, and mass fractions that are obtained by the line shape analysis are listed for the crystalline, interfacial, and rubbery components. The chemical shift values stay constant in this temperature region for all the crystalline components, while those values of the interfacial and rubbery components shift somewhat upfield with increasing temperature. This fact indicates the increase

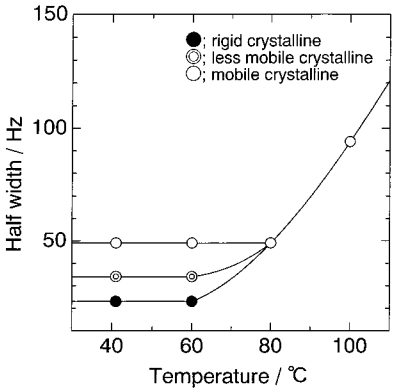

Figure 2. Half-width versus temperature for each crystalline component in MLLDPE.

Table 2. NMR Relaxation Parameters for MLLDPE at Different Temperatures

	crystalline (orthorhombic)			noncrystalline	
	rigid	less mobile	mobile	interfacial	rubbery
41 °C					
chemical shift/ppm	32.9	32.9	32.9	31.0	30.7
T_{1C}/s	288	25	1.4	0.41	0.41
half-width/Hz	23	34	49	100	44
mass fractions	0.21	0.15	0.14	0.41	0.09
60 °C					
chemical shift/ppm	32.9	32.9	32.9	30.8	30.5
T_{1C}/s	217	21	1.8	0.51	0.51
half-width/Hz	23	34	49	74	29
mass fractions	0.19	0.16	0.15	0.30	0.19
80 °C					
chemical shift/ppm	32.9	32.9	32.9	30.7	30.4
T_{1C}/s	111	12	0.88	0.59	0.59
half-width/Hz	49	49	49	61	20
mass fractions	0.17	0.15	0.15	0.27	0.26
100 °C					
chemical shift/ppm	32.9	32.9	32.9	30.6	30.4
T_{1C}/s	72	5.6	0.93	0.59	0.59
half-width/Hz	94	94	94	56	16
mass fractions		0.41		0.18	0.41

in fraction of the gauche conformation for the respective noncrystalline components. When the γ-gauche effect and the vicinal gauche effect are respectively assumed to be 5.0 and 2.5 ppm,[29] gauche fractions in the interfacial and rubbery components are increased by 0.27 and 0.20 at 100 °C compared to those at 41 °C, respectively. T_{1C} values for the respective components are also shown in Table 2. It is found that the T_{1C} value of each crystalline component is remarkably decreased with increasing temperature, reflecting the enhanced molecular motion as well as the possible increase in chain diffusion rate.

Figure 2 shows the temperature dependency of the half-width of the resonance line for each crystalline component of MLLDPE obtained by the line shape analysis. Interestingly, these three components with different T_{1C} values have also different half-widths at 41−60 °C, indicating that these components really have different molecular mobilities in this temperature region. However, their half-widths are in accord with each other at 80 °C as a result of broadening for the rigid and less mobile crystalline components and are further increased with increasing temperature. Such marked broadening above 80 °C implies that the molecular motion of the crystalline chains moves into the range of the rates of about 10^5 Hz which corresponds to ^{1}H dipolar decoupling field.[16−18] In our previous work,[30] the line width of the crystalline component was also measured as a function of the amplitude of dipolar decoupling field for a similar LLDPE sample at 80 and 100 °C. Although remarkable amplitude dependencies were observed at both temperatures, the explicit rate of the motion was not determined because of the difficulty in measuring the further narrowing process. However, the order of the rate was confirmed to be about 10^5 Hz in this temperature region. It should be also noted here that this molecular motion is allowed to occur above 60 °C at almost the same level in every crystalline region. The mode of the molecular motion to interpret this phenomenon will be described later.

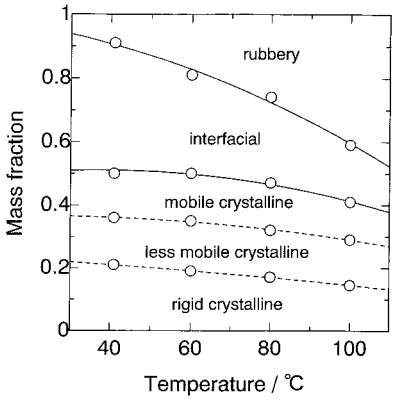

Figure 3. Partitioning (by differences) of the various mass fractions for each component in MLLDPE as a function of temperature.

In Figure 3 the mass distribution diagram of MLLDPE is shown as a function of temperature. The rubbery component remarkably increases in mole fraction with the increase of temperature, mainly as a result of the decrease in fraction of the interfacial component. According to the theory[20] derived by using the lattice model, the interfacial region is defined as a transitional region where the restriction due to the fixation of chain ends on the surface of crystallites still exists for the conformational probability. However, since this definition is held in the thermodynamically equilibrium state,[20] the average by molecular motion will reduce such conformational restriction particularly for NMR relaxation parameters. As a result, the interfacial component seems to change to the rubbery component with increasing temperature.

As for the crystalline region, the total mass fraction of this component is slightly decreased above 60 °C with increasing temperature. This fact is in good accord with the appreciable detection of partial melting above 60 °C by DSC[1] and may be associated with surface melting of the crystallites observed by small-angle X-ray scattering experiments.[31] In contrast, when the resonance line of the crystalline component was assumed to be a single Lorentzian curve in the line shape analysis shown in Figure 1, the degree of crystallinity was found to stay constant in this temperature region unlike the result shown in Figure 3 and the DSC measurements. This fact also supports the existence of plural crystalline components with different molecular mobilities and the validity of the line shape analysis based on them. As is clearly seen in Figure 3, each crystalline component gradually decreases above 60 °C. The rigid crystalline component converts to the less mobile crystalline component, the latter to the mobile, and then the mobile

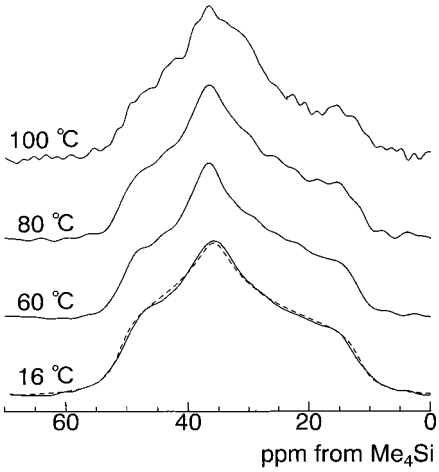

Figure 4. ^{13}C CSA spectra of the crystalline component of MLLDPE at different temperatures: solid line, observed; dashed line, simulated in the rigid state.

crystalline component to the interfacial component. Such conversion will be also associated with the chain diffusion as well as the decrease in lamellar thickness due to the surface melting.

Judging from the temperature dependence of the line width shown in Figure 2, the mobile crystalline component is much mobile than the rigid crystalline and less mobile crystalline components below 80 °C. The origin of the mobile crystalline component is considered to be the surface component of the crystalline lamellae[31] or small size crystals.[1]

It is also noted that no change is observed in line width of the rigid crystalline and the less mobile crystalline component from 41 to 60 °C and that of the mobile crystalline component from 41 to 80 °C. In contrast, slight line broadening in high-resolution ^{13}C NMR spectra was observed even from room temperature for conventional polyethylene single crystals,[30] as-polymerized polyethylenes,[15] and bulk-crystallized polyethylenes.[15] It is reported that slowly crystallized metallocene-catalyzed LLDPE shows unprecedented stability in that its morphology is invariant even after high-pressure crystallization.[24] The temperature dependency of the half-width shown in Figure 2 is considered to reflect almost no significant change in local structure associated with such morphological stability for slowly crystallized metallocene-catalyzed LLDPEs.

180° Flip Motion in the Crystalline Region. To clarify the mode of the molecular motion for the crystalline component with about 10^5 Hz above 60 °C, ^{13}C CSA has been selectively measured for the crystalline component at 16−100 °C by using the CPT1 pulse sequence with the T_{1C} decay time of 2.0 s. In these spectra, the interfacial and rubbery components disappear due to their short T_{1C} values. Some fractions of the mobile and less mobile components are also suppressed in the CSA spectra, but the features of the molecular motion associated with the line broadening shown in Figure 2 will be well reflected because this motion is allowed to occur in the whole crystalline region. Figure 4 shows ^{13}C CSA spectra thus obtained for the crystalline component of MLLDPE at different temperatures. Here, the broken line indicates the simulated CSA spectrum for the polyethylene orthorhombic crystals in the rigid state, where the principal values of $\sigma_{11} = 50.7$ ppm, $\sigma_{22} = 35.9$ ppm, and $\sigma_{33} = 12.1$ ppm were employed on the basis of the previous publications.[32−34] As expected, the ^{13}C CSA line shape at 16 °C is in good accord with the line shape in the rigid state. Interestingly, this line shape is not significantly changed even above 60 °C, although marked motional broadening is observed above this temperature in the DD/MAS ^{13}C NMR spectra as shown in Figure 2.

The assignment for the principal axes of the chemical shift tensor for the CH_2 carbon of polyethylene was made for the rigid orthorhombic crystals:[32−35] The σ_{11} axis is parallel to the intra-methylene H−H vector, the σ_{22} axis to the H−C−H angle bisector, and the σ_{33} axis to the molecular chain axis. According to this assignment, it is most plausible to conclude that the 180° flip motion around the molecular chain axis[2,6,7,15] occurs above 60 °C with the rate of about 10^5 Hz in the crystalline region. The CSA spectrum is insensitive to this motion, but it will be able to modulate the ^1H dipolar decoupling field, resulting in marked line broadening for CP/MAS ^{13}C spectra as shown in Figure 2.

A recent work[14] about measurements of the $^{13}C-^{13}C$ dipolar coupling also confirmed more directly the existence of the 180° flip motion in the crystalline region of polyethylene in a similar temperature region. However, in that work, the rate of 180° flip motion was determined to be about 10^3 Hz at 80 °C. Moreover, significant broadening of the crystalline resonance line in the CP/MAS ^{13}C NMR spectrum due to the 180° flip motion was observed above about 100 °C for constrained ultradrawn polyethylene fibers.[19] These facts indicate that the rate of 180° flip motion at a given temperature depends on the structure of polyethylene samples used.

It should be simply noted here that there are slight deviations for the CSA spectra at 60−100 °C from the CSA spectrum in the rigid state. This fact suggests that the enhanced twisting motion along the molecular chain axis[7,36−38] and/or local motion associated with small defects[39,40] may be induced at higher temperatures in addition to the 180° flip motion around the chain axis. At this stage, however, it seems beyond the purpose of this paper to analyze the ^{13}C CSA line shape by considering such twisting or small defects.

Characterization of the Chain Diffusion by 2D ^{13}C Exchange NMR. The 180° flip motion around the chain axis in the orthorhombic phase for polyethylene should really involve the concomitant translational motion by one methylene unit.[2,6,7,12,14] If forward and backward 180 ° flip motions would successively occur as multistep jumps, the crystalline and noncrystalline segments could exchange as a result of the translational motion of the chains along the molecular chain axis. In fact, for an as-polymerized sample of high-density polyethylene, the segment exchange was observed between the crystalline and noncrystalline regions by using 2D exchange ^{13}C NMR spectroscopy.[12] It is interesting to examine whether butyl branches hinder the exchange between the crystalline and noncrystalline segments because butyl branches should not be included in the crystalline region.[1,24] Moreover, the real correlation between the 180° flip motion and the chain diffusion inducing the segmental exchange of the crystalline and noncrystalline components should be evaluated here somewhat in detail.

Figure 5 shows the 2D exchange ^{13}C NMR spectrum of MLLDPE12 obtained at 80 °C under the DD/MAS condition without using the CP technique, with a mixing time of 1 s and a recycle delay of 5 s. Two cross-peaks are clearly observed together with two larger diagonal

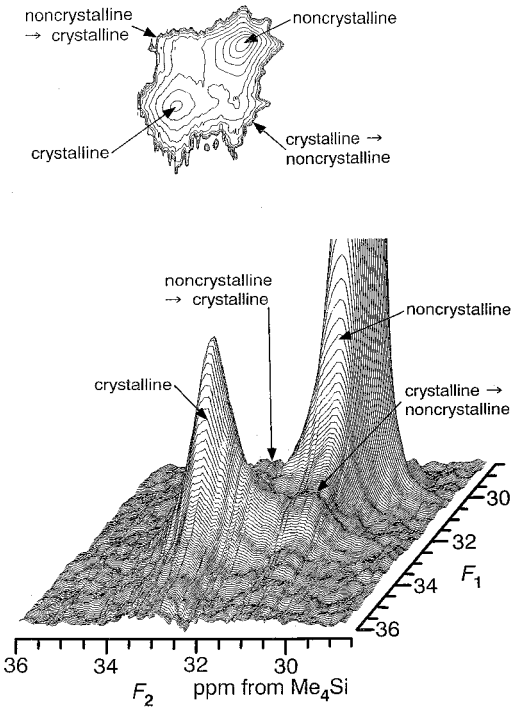

Figure 5. DD/MAS 2D exchange ^{13}C NMR spectrum measured for MLLDPE12 at 80 °C, with a mixing time of 1 s and a recycle delay of 5 s.

peaks assigned to the crystalline and noncrystalline components. Since the ^{13}C spin diffusion contribution to the cross-peaks can be excluded under the present experimental condition as previously discussed in detail,[12] the appearance of the cross-peaks really indicates the segmental exchange between the crystalline and noncrystalline regions for MLLDPE12 with butyl branches.

The intensity of the resonance line for the crystalline component transferred from the noncrystalline region within 1 s has been estimated to be 0.10 against the total noncrystalline resonance line as an average integrated fraction for five slice spectra along the F_2 axis including the cross crystalline and diagonal noncrystalline lines. Considering the T_{1C} effects during the mixing time (see Appendix), the real mole fraction of the crystalline component transferred from the noncrystalline region within 1 s has been estimated to be in the range 0.074−0.13 against the total noncrystalline component.

A similar 2D exchange ^{13}C NMR measurement was also performed at 90 °C. However, no increase in intensity was observed for the cross-peak of the crystalline component transferred from the noncrystalline region. Since the translational molecular motion along the chain axis is considerably restricted by the fact that butyl branches cannot enter the crystalline region,[1] each chain should go forward and backward many times between the limited crystalline and noncrystalline regions during the mixing time. In this respect, the increase in mobility at a higher temperature is not directly correlated with the increase in intensity of the cross-peak for this LLDPE sample.

A Random Walk Simulation for the Chain Diffusion. To evaluate the level of the fraction of the crystalline component transferred from the noncrystalline region, a simple simulation has been made by using a random walk model for the chain diffusion due to the multistep forward and backward 180° flip motions. A Monte Carlo simulation was already made in detail for the chain diffusion in linear polyethylene lamellar crystals with noncrystalline loops.[12] However, the contribution of short branches was not considered as yet. Here, we simulate the chain diffusion process by using the one-dimensional random walk model, considering the multistep forward and backward 180° flip motions for the linear low-density polyethylene sample with butyl branches.

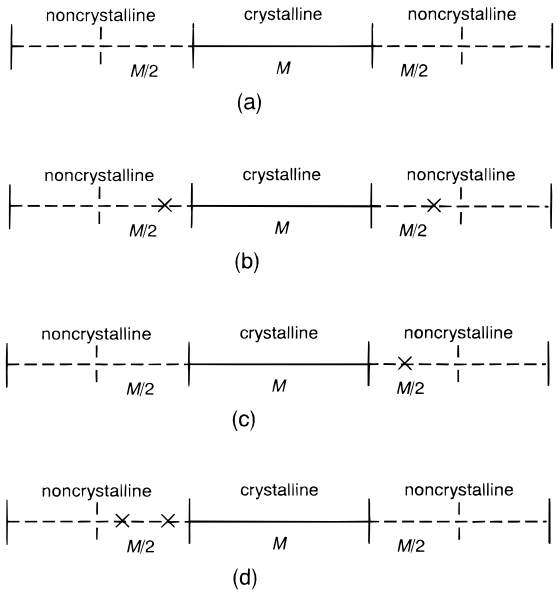

Figure 6. Schematic structural model of the one-dimensional random walk for the chain diffusion. The character "×" indicates a butyl branch. The character "*M*" denotes the number of methylene units.

The assumptions made for the simulation are as follows: (1) Both the crystalline stem and noncrystalline sequence consist of *M* CH_2 units as shown in Figure 6a−d, and the degree of crystallinity (0.50) stays constant. The value *M* can be determined from the lamellar thickness (8.9 nm)[1] and the angle between the *c*-axis and the lamellar normal (35°).[24] (2) Butyl branches are equally distributed in the noncrystalline regions without entering the crystalline region.[1] (3) The 180° flip motions induce forward and backward CH_2 movements, which correspond to steps for the one-dimensional random walk, along the chain axis in the crystalline region. (4) The probabilities for the respective forward and backward steps are 0.50 for the chain diffusion, which is really described in terms of the one-dimensional random walk model. (5) The number of steps of the random walk is *N*, which will be determined by (rate of the 180° flip) × (mixing time). (6) The 180° flip motion is assumed to be independently induced in each crystalline stem, and the density should not be greatly changed from the averaged value in the noncrystalline region. Therefore, the net movement of the originally crystalline stem may be limited within a certain area from the surface of the crystallite. For simplicity, it is here assumed that the terminal CH_2 in the crystalline region will be allowed to move to the middle of the noncrystalline sequence (*M*/2). This assumption is also supported by the fact that butyl branches cannot enter the crystalline region. In this respect, long-range correlations between the displacements of different chain stems[12,13] are neglected for this LLDPE sample. (7) The noncrystalline overlayer of the polyethylene single crystals was

found to be mainly composed of loose loops,[21] and it was also beyond the limit of the solid-state NMR detection to observe the contribution from the folding CH_2 carbons in our isothermally crystallized LLDPE. Therefore, the fraction of sharp folds is assumed to be negligible in this calculation. Since a similar NMR analysis of the polyethylene single crystals with loose loops will be published somewhere, detailed discussion about the sharp folds will be made there.

The mole fraction $F(N)$ of the CH_2 units transferred from the crystalline region to the noncrystalline region within a given time against the total CH_2 units is given by

$$F(N) = {}^1/_2 \sum_{n \neq 0} f(n) \tag{1}$$

when each original crystalline stem is transferred as a whole from the initial crystalline region. Here, $f(n)$ is the mole fraction for the CH_2 units that move by n CH_2 units from the surface of the crystalline region after N steps. The probability $P(n)$ for the CH_2 units that move by n CH_2 units along the chain from the initial position after N steps is given by

$$P(n) = ({}^1/_2)^N N!/[(N+n)/2]![(N-n)/2]! \tag{2}$$

where n covers the limited numbers according to the cases described below. Positive and negative numbers for n in eq 2 correspond to the movements to the right and left directions in each case shown in Figure 6, respectively. The normalization of $P(n)$ is carried out depending on the conditions of the simulation as described below. Since $f(n) = |n|P(n)/M$, eq 1 is expressed as

$$F(N) = \sum_{n \neq 0} |n| P(n)/2M \tag{3}$$

For simplicity, N is assumed to be much larger than n because the rate of the 180° flip motion which corresponds to N is about 10^5 Hz. Judging from eq 2, therefore, $P(n)$ may be independent of n, resulting in $P(n) = 1/(M_a + 1)$. Here, M_a is the number of the sites in the noncrystalline region to which the crystalline stem can be transferred.

Figure 6a−d shows schematic models for distributions of butyl branches (x) assumed in this simulation. Here, since the mole fraction of the branches is of the order of 0.01, the four following cases are assumed depending on the positions of branches in the noncrystalline region.

Case A: No Branches in Both Noncrystalline Regions with *M*/2 CH_2s (Figure 6a). In this case, the crystalline stem can move in the whole noncrystalline range of $M/2 \geq n \geq -M/2$. Since $P(n) = 1/(M+1)$, F_A corresponding to $F(N)$ in case A is given by

$$F_A = \sum_{n=-M/2}^{M/2} |n|/[2M(M+1)] = (M+2)/[8(M+1)] \tag{4}$$

Case B: One Branch in Both Noncrystalline Regions (Figure 6b). The noncrystalline CH_2 units are hereafter referred to as m_l or m_r (l, r = 1, 2, ..., $M/2$) from the crystalline stem end. When the butyl branches exist at m_l and m_r, n should be $-m_{r-1} \leq n \leq m_{l-1}$. In this case $f(n)$ is given by

$$f(n) = \sum_{n=-m_{r-1}}^{m_{l-1}} |n|/[2M(m_l + m_r - 1)] = [m_l(m_l-1) + m_r(m_r-1)]/[4M(m_l + m_r - 1)] \tag{5}$$

Therefore, F_B is expressed as

$$F_B = (2/M)^2 \sum_{m_r=1}^{M/2} \sum_{m_l=1}^{M/2} [m_l(m_l-1) + m_r(m_r-1)]/[4M(m_l + m_r - 1)] \tag{6}$$

Cases C and D: One Branch and Two Branches in Either Noncrystalline Region (Figure 6c,d). In a similar way, $f_C(n)$ and $f_D(n)$ are respectively derived in cases C and D as follows:

$$f_C(n) = \sum_{n=-m_{r-1}}^{M/2} |n|/[M(M+2m_r)] = [M(M+2) + 4m_r(m_r-1)]/[8M(M+2m_r-2)] \tag{7}$$

$$f_D(n) = \sum_{n=-m_{r-1}}^{0} [|n|(M/2-|n|)]/[M(M+2m_r-2)(M/2)] = (3M - 4m_r + 2)m_r(m_r-1)/[6M^2(M+2m_r-2)] \tag{8}$$

Then,

$$F_C = (2/M) \sum_{m_r=1}^{M/2} [M(M+2) + 4m_r(m_r-1)]/[8M(M+2m_r-2)] \tag{9}$$

$$F_D = (2/M) \sum_{m_r=1}^{M/2} [(3M - 4m_r + 2)m_r(m_r - 1)/\{6M^2(M+2m_r-2)\} + (M+2)/\{8(M+2m_r-2)\}] \tag{10}$$

Next, we derive equations for the probabilities for cases a−d. When one branch is assumed to exist per b CH_2 units, the respective probabilities P_A, P_B, P_C, and P_D for cases A, B, C, and D are straightforwardly given as

$$P_A = (1-2/b)^{M/2\times 2} = (1-2/b)^M$$

$$P_B = [(1-2/b)^{M/2-1}(2/b)(M/2)]^2 = (1-2/b)^{M-2}(M/b)^2$$

$$P_C = 2(1-2/b)^{M/2}[(1-2/b)^{M/2-1}(2/b)(M/2)] = 2(1-2/b)^{M-1}(M/b)$$

$$P_D = 2(1-2/b)^{M/2}[(1-2/b)^{M/2-2}(2/b)^2(M/2)(M/2-1)/2] = (1-2/b)^{M-2}(M/b^2)(M-2) \tag{11}$$

Consequently, the total mole fraction F_T of CH_2 units that move from the crystalline region to the noncrystalline region is given by

$$F_T = (P_A F_A + P_B F_B + P_C F_C + P_D F_D)/(P_A + P_B + P_C + P_D) \tag{12}$$

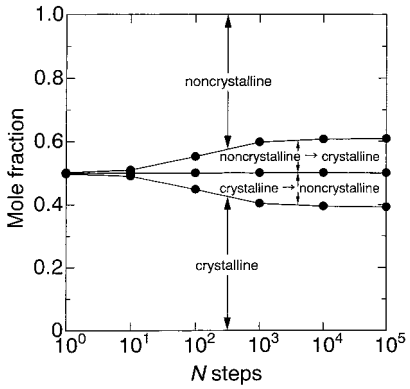

Figure 7. Mole fraction versus number N of steps per second for each component for polyethylene.

According to the experimental results described above, $N = 10^5$, $b = 100$, and $M = 88$. Therefore, the numerical calculation by a computer reveals $F_T = 0.108$. Since the degree of crystallinity is assumed to stay constant in this simulation, the same fraction of the noncrystalline component is transferred to the crystalline region. Finally, the fraction of the CH_2 carbons transferred from the noncrystalline region to the crystalline region against the total CH_2 carbons in the noncrystalline region can be determined as 0.22. Interestingly, this calculated value is larger by 2−3 times than the value (0.074−0.13) experimentally obtained in Figure 5. This suggests that all 180° flip motions may not simply contribute to the chain diffusion along the chain axis in the crystalline region.

A similar simulation has separately been made by using the probability $P(n)$ exactly described in terms of eq 2, and the mole fraction of each component obtained by this simulation is plotted against the number N of steps in Figure 7. Here, the normalization of $P(n)$ was numerically conducted for $M/2 \geq n \geq -M/2$ in the computer calculation process. This figure clearly reveals that F_T is significantly decreased with decreasing N. According to this result, F_T is reduced from 0.11 for $N = 10^5$ to about 0.05 for $N = \sim 3 \times 10^2$. This indicates that the mole fraction of the crystalline component transferred from the noncrystalline region against the total noncrystalline component is about 0.1 for $N = \sim 3 \times 10^2$, which is in good accord with the value experimentally obtained. It will be, therefore, plausible to point out that the number of steps for the chain diffusion may be reduced to the order of 3×10^2 for MLLDPE12, although this value is greatly lower compared to the rate of 10^4−10^5 Hz for the 180° flip motion. This suggests that the 180° flip motion may be mostly the two-site forward and backward motion, and only about 1% of the flip motion will contribute to the chain diffusion along the chain axis. In addition, the diffusion coefficient D can be estimated to be ~ 2.3 nm^2 s^{-1} by using the relation $D = \lambda^2 N/2t_m$, where λ is the step distance (=0.125 nm) and t_m is the mixing time (=1 s). This value is somewhat larger compared to the D values previously obtained by the T_{1C} relaxation analysis.[13] Moreover, the average chain diffusion distance described as the number of CH_2 carbons is estimated to be about 17 CH_2 carbons per second.

An alternative possible explanation of the larger simulated value for F_T may be the overestimation of the noncrystalline region that the crystalline chain is allowed to diffuse. In fact, when $M/2$ is reduced to $M/4$ for the noncrystalline region shown in Figure 6, the F_T value is found to be about 0.05, in good accord with the experimental result shown in Figure 5. In this case, therefore, the chain diffusion rate should be of the order of the rate of 180° flip motion. The confirmation of the real mechanism of the chain diffusion will need the direct measurement of the diffusion coefficient D along the molecular chain axis.

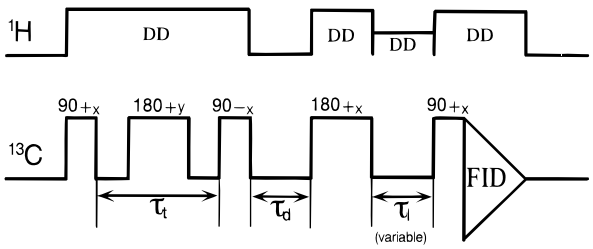

Figure 8. Pulse sequence prepared by the combination of the Goldman−Shen pulse sequence modified for ^{13}C measurements and the inversion recovery method in the solid state.

^{13}C Spin−Lattice Relaxation Behavior for the Crystalline Component Transferred from the Noncrystalline Region. As described above, there are three crystalline components with different T_{1C} values for this sample in accord with the previous results for different polyethylene samples.[1,21−23] It would be interesting to examine which crystalline component may be assigned to the component transferred from the noncrystalline region within 1 s. Figure 8 shows the pulse sequence originally prepared for the T_{1C} measurement of the component transferred from the noncrystalline region to the crystalline region. The pulse sequence, combined with the Goldman−Shen pulse sequence[41] modified for ^{13}C measurements and the inversion recovery method in the solid state, is composed of four periods. The first is the preparation period (τ_t), in which the ^{13}C magnetization is created using the difference in ^{13}C spin−spin relaxation times (T_{2C}) of the respective components. At the end of this period, there exists only the magnetization of the rubbery amorphous component, which has a longer T_{2C} value. The second is the diffusion period (τ_d), during which the rubbery component set parallel to the $+z$ axis diffuses to the crystalline region. The third is the ^{13}C spin−lattice relaxation period (τ_l), in which the ^{13}C magnetization is flipped to the $-z$ axis and is relaxed to the equilibrium value. The fourth is the detection period.

First, we have measured T_{1C} values for the respective components of MLLDPE12 at 80 °C by the conventional CPT1 pulse sequence.[25] The crystalline component has three different T_{1C} values with $T_{1C} = 171$, 29, and 1.9 s at 80 °C, while the noncrystalline component has only a single component with $T_{1C} = 1.2$ s. These T_{1C} values obtained are shown in Table 3.

Figure 9 shows partially relaxed ^{13}C NMR spectra for MLLDPE12 at $\tau_t = 50$ ms and $\tau_d = 1$ s obtained by the pulse sequence shown in Figure 8. The character "b" indicates the resonance lines from butyl branches. The thick arrow denotes the resonance line at 32.9 ppm which partly contains the crystalline component produced by the chain diffusion from the noncrystalline region during the mixing time τ_d. This resonance line also contains the contribution of the crystalline component produced by the normal T_{1C} relaxation during the period of τ_d.

Figure 10 shows the plot for the peak intensity of the resonance line at 32.9 ppm shown in Figure 9 against the delay time τ_l for the T_{1C} relaxation. The solid line

Table 3. T_{1C} Values for MLLDPE12 at 80 °C

	crystalline (orthorhombic)			the component produced by the chain diffusion from the noncrystalline to the crystalline region	noncrystalline	
	rigid	less mobile	mobile		interfacial	rubbery
T_{1C}/s	171[a]	29[a]	1.9[a]	2.0[b]	1.2[a]	1.2[a]

[a] Determined by the CPT1 measurements. [b] Determined by the pulse sequence shown in Figure 8.

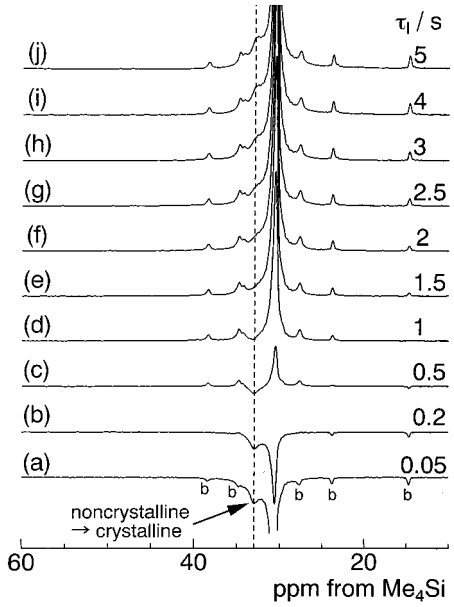

Figure 9. Partially relaxed ^{13}C NMR spectra measured for MLLDPE12 at 80 °C by the pulse sequence shown in Figure 8, with $\tau_t = 50$ ms and $\tau_d = 1$ s. The thick arrow denotes the crystalline component transferred by the chain diffusion from the noncrystalline region. The character "b" indicates the resonance line from butyl branches.

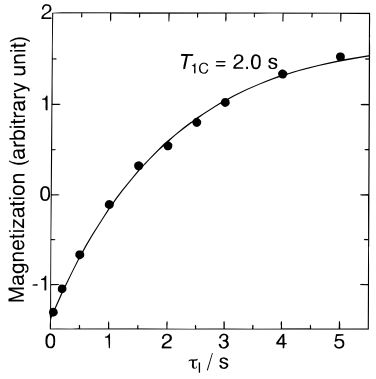

Figure 10. Inversion recovery process for the resonance line produced by the chain diffusion from the noncrystalline region as shown in Figure 9.

is the calculated result obtained by the least-squares method by assuming a single-exponential T_{1C} decay. As is clearly seen, this relaxation process can be described by a single component with a T_{1C} value of 2.0 s. This fact suggests that the crystalline component transferred from the noncrystalline region through the chain diffusion within 1 s has the same T_{1C} value (2.0 s) as that for the crystalline component produced by the normal T_{1C} relaxation during the τ_d period. To confirm this suggestion, a similar line shape analysis that is shown in Figure 1 was carried out for the spectrum for $\tau_l = 0.05$ s shown in Figure 9a. In this case, a single Lorentzian curve was employed for the crystalline component. A resulting good fit revealed that the mass fractions of the CH_2 carbons in the crystalline, interfacial, and rubbery regions are 0.31, 0.30, and 0.39, respectively. According to the 2D exchange spectrum shown in Figure 5, the fraction of the crystalline component transferred from the noncrystalline region within 1 s is about 0.10 against the total noncrystalline component. Using this value,[42] the fraction of the crystalline component transferred from the noncrystalline region was approximately estimated to be about 0.07 ($\cong(0.30 + 0.39) \times 0.1$) for the CH_2 resonance line in Figure 9a where the line shape analysis described above was performed. Therefore, the fraction of this component in the T_{1C} relaxation process shown in Figure 10 is found to be as significantly high as 0.23 (=0.07/0.31) compared to the fraction of 0.77 for the normal T_{1C} relaxation component. This level of the fraction is highly enough to determine the reliable T_{1C} value for this component. In fact, no good fit was obtained for the T_{1C} relaxation process when another possible T_{1C} value of 29 or 171 s was introduced. It is, therefore, concluded that the crystalline component transferred from the noncrystalline region within 1 s has a T_{1C} value of 2.0 s. This indicates that the mobile crystalline component with $T_{1C} = 1.9$ s is allowed to exchange within 1 s with the noncrystalline component through the chain diffusion associated with the multistep 180° flip motions.

Judging from the temperature dependence of the line width shown in Figure 2, the rigid crystalline and less mobile crystalline components should be also associated with the 180° flip motion above 60 °C, but these components are not allowed to exchange with the noncrystalline component within 1 s. Such a limitation will be interpreted by the location of these components in the crystallites; the most outer part or the surface area of the crystallite along the chain axis should be composed of the mobile crystalline component, whereas the inner and core parts will consist of the less mobile and rigid crystalline components. This structure model may be also supported by the short average diffusion distance that was estimated to be about 17 CH_2 units (~21 nm) by the simulation results as described above. The reason is that this diffusion distance is of almost the same order of the thickness (~18 nm) of the mobile crystalline component which is estimated from the mass fraction shown in Table 2 and the total thickness (8.9 nm) of the crystallite by assuming its existence at both surfaces of the crystallite. The previous work also revealed that the shorter T_{1C} component, which would be located near the surface of the crystallite, gave the larger cross-peaks in 2D exchange ^{13}C NMR spectra.[12]

According to this structural model, the existence of three components with different T_{1C} values above 80 °C can be also reasonably interpreted as follows: Since the 180° flip motion is the overall motion of the crystalline stem composed of the three components, line broadening induced as a result of the modulation of the ^1H dipolar decoupling field by this motion is almost of the same level for each component. In contrast, the local motional fluctuation around the C−C bond, which determines the T_{1C} value through the spectral density of about 10^8 Hz, and the extent of the average of T_{1C} by the chain

diffusion may be still greatly different above 80 °C in these three components possibly depending on the level of disordering and the location in crystallites.

Conclusions

The crystalline−noncrystalline structure and molecular motion of metallocene-catalyzed linear low-density polyethylene (MLLDPE) have been investigated in the α relaxation temperature region by solid-state ^{13}C NMR spectroscopy, and the following conclusions have been obtained:

(1) Fully relaxed high-resolution solid-state ^{13}C NMR spectra are reasonably resolved into the crystalline, crystalline−amorphous interfacial, and rubbery amorphous components at different temperatures above room temperature. Prominent temperature dependencies are observed for the mass fractions, T_{1C} values, and line widths of the three components. Moreover, marked broadening of the resonance line for the crystalline component above 60 °C and no change in its CSA line shape confirm, in good accord with the previous results, that the 180° flip motion around the chain axis with about 10^5 Hz occurs in the whole crystalline region in MLLDPE with butyl branches.

(2) Although about 10 butyl branches per 1000 CH_2 carbons are distributed in the noncrystalline region for MLLDPE, the two-dimensional ^{13}C exchange NMR spectrum measured at 80 °C clearly reveals the segmental exchange between the crystalline and noncrystalline regions due to the chain diffusion along the chain axis. The mole fraction of the crystalline component transferred from the noncrystalline region within 1 s is estimated to be 0.074−0.13 against the total noncrystalline component.

(3) The one-dimensional random walk simulation closely relating to the multistep forward and backward 180° flip motions is carried out for polyethylene with butyl branches that are statistically distributed in the noncrystalline region to evaluate the chain diffusion process along the chain axis observed by 2D ^{13}C exchange NMR spectroscopy. The mole fraction of the crystalline component transferred from the noncrystalline region within 1 s is determined to be 0.22, which is 2−3 times larger than the value experimentally obtained. The cause of such a discordance between the experimental and simulated results may be due to the much lower elementary-step rate for the chain diffusion compared to the rate (∼10^5 Hz) of the 180° flip motion. An alternative explanation will be also possible by considering the spatial limitation for the noncrystalline region where the crystalline chains are allowed to diffuse.

(4) The T_{1C} value for the crystalline component transferred by the chain diffusion from the noncrystalline region within 1 s is found to correspond to the shortest T_{1C} value among the three T_{1C} values in the crystalline components. This fact indicates that the crystalline component with the shortest T_{1C} value should be assigned to the surface component of the crystallite that is closely associated with the segmental exchange between the crystalline and noncrystalline region. This finding also seems to be in good accord with the short diffusion distance that is estimated from the possible small number of elementary diffusion steps for the simulation of the chain diffusion.

Acknowledgment. We thank Professor David C. Bassett and Dr. Robert H. Olley of J. J. Thomson Physical Laboratory in University of Reading for providing the linear low-density polyethylene sample. We are also grateful to Mr. Yoshihiro Motegi of Japan Polyolefins Co. Ltd. for kindly supplying the linear low-density polyethylene sample CX507#12.

Appendix: T_{1C} Effects on the Mole Fraction of the Crystalline Component Transferred from the Noncrystalline Component

As described in the text, the mole fraction of the crystalline component transferred from the noncrystalline component was experimentally estimated to be 0.10 against the total noncrystalline component. Strictly speaking, this value is not accurately determined because T_{1C} effects are not considered during the spin exchange process within a period of 1 s. Here, we evaluate the T_{1C} effects on the fraction of the transferred crystalline component to obtain the corrected mole fraction.

In the pulse sequence used for the measurement of the DD/MAS 2D exchange ^{13}C spectrum shown in Figure 5, the ^{13}C magnetization is alternatively set parallel to the $+z$ or $-z$ axis just before the mixing period. After the mixing period of τ_d the difference of the magnetizations obtained by the respective settings are accumulated as free induction decays. Therefore, the magnetizations M_c and M_n of the crystalline and noncrystalline components after the two-dimensional Fourier transformation are given by

$$M_c = M_{c0} \exp(-\tau_d/T_{1Cc}) \quad \text{(A1)}$$

$$M_n = M_{n0} \exp(-\tau_d/T_{1Cn}) \quad \text{(A2)}$$

when no chain diffusion occurs between the crystalline and noncrystalline components. Here, M_{c0} and M_{n0} are the magnetizations of the crystalline and noncrystalline components used by the initial 90° pulse in the 2D exchange pulse sequence, respectively. T_{1Cc} and T_{1Cn} are the T_{1C} values of the crystalline and noncrystalline components. If the segmental exchange occurs between these two components by the chain diffusion, we need detailed information about the periods of stays in the two regions for the respective ^{13}C nuclei. The calculation may be carried out statistically, but it will be beyond the scope of this paper because of the complexity. Therefore, the maximum and minimum effects of T_{1C} during the mixing time are evaluated as follows.

In the case of the crystalline component transferred from the noncrystalline region, this component is assumed to be transferred just after $\tau_d = 0$ and to stay in the crystalline region during the mixing time. Then, the minimum correction factor for the intensity of the cross-peak for the crystalline component may be $\exp(\tau_d/T_{1Cc})$. In contrast, the maximum correction factor will be $\exp(\tau_d/T_{1Cn})$, which corresponds to the case where the transfer is completed just before the end of the mixing time. In the usual measurements, we observe the average of the crystalline component which is finally transferred from the original noncrystalline component after some exchanges between these two components during the mixing time. Accordingly, the actual correction factor will be a certain averaged value between the maximum and minimum values. On the other hand, the noncrystalline component appearing as a diagonal peak should contain the component that comes back from the crystalline region after some stays for certain periods

during the mixing time. Although the amount of this component may be small in our polyethylene sample, the maximum and minimum correction factors for the diagonal noncrystalline component will be respectively estimated as $\exp(\tau_d/T_{1Cn})$ and $\exp(\tau_d/T_{1Cc})$ in a similar way to the case for the crystalline component described above.

As a result, the corrected mole fraction $I_{nc0}/(I_{nc0} + I_{n0})$ for the crystalline component transferred from the noncrystalline region during the τ_d period is given by the following inequality expression:

$$I_{nc}\exp(\tau_d/T_{1Cn})/[I_{nc}\exp(\tau_d/T_{1Cn}) + I_n\exp(\tau_d/T_{1Cc})] > I_{nc0}/(I_{nc0} + I_{n0}) > I_{nc}\exp(\tau_d/T_{1Cc})/[I_{nc}\exp(\tau_d/T_{1Cc}) + I_n\exp(\tau_d/T_{1Cn})] \quad \text{(A3)}$$

Here, I_n and I_{nc} are the intensities of the diagonal noncrystalline peak and the cross crystalline peak observed in the 2D exchange ^{13}C spectrum with the mixing time of τ_d, respectively. Since $I_{nc}/I_n = 1/9$, $T_{1Cc} = 1.9$ s, $T_{1Cn} = 1.2$ s, and $\tau_d = 1$ s, eq A3 reduces to

$$0.13 > I_{nc0}/(I_{nc0} + I_{n0}) > 0.074 \quad \text{(A4)}$$

References and Notes

(1) Kuwabara, K.; Kaji, H.; Horii, F.; Bassett, D. C.; Olley, R. H. *Macromolecules* **1997**, *30*, 7516.
(2) McCrum, N. G.; Read, B. E.; Williams, G. *Anelastic and Dielectric Effects in Polymer Solids*; Wiley: New York, 1967.
(3) Nakayasu, H.; Markovitz, H.; Plazek, D. *J. Trans. Soc. Rheol.* **1961**, *5*, 261.
(4) Cembrola, R. J.; Stein, R. S. *J. Polym. Sci., Polym. Phys. Ed.* **1980**, *18*, 1065.
(5) Takayanagi, M.; Matsuo, T. *J. Macromol. Sci., Phys.* **1967**, *B1*, 407.
(6) Boyd, R. H. *Polymer* **1985**, *26*, 323.
(7) Boyd, R. H. *Polymer* **1985**, *26*, 1123.
(8) Matsuo, M.; Sawatari, C.; Ohhata, T. *Macromolecules* **1988**, *21*, 1317.
(9) Ohta, Y.; Yasuda, H. *J. Polym. Sci., Polym. Phys. Ed.* **1994**, *32*, 2241.
(10) For example: (a) Horii, F.; Kaji, H.; Ishida, H.; Kuwabara, K.; Masuda, K.; Tai, T. *J. Mol. Struct.* **1998**, *441*, 303. (b) Nakaoki, T.; Ohira, Y.; Hayashi, H.; Horii, F. *Macromolecules* **1998**, *31*, 2705.
(11) VanderHart, D. L. *J. Magn. Reson.* **1987**, *72*, 13.
(12) Schmidt-Rohr, K.; Spiess, H. W. *Macromolecules* **1991**, *24*, 5288.
(13) Robertson, M. B.; Ward, I. M.; Klein, K. G.; Packer, K. J. *Macromolecules* **1997**, *30*, 6893.
(14) Hu, W. -G.; Boeffel, C.; Schmidt-Rohr, K. *Macromolecules* **1999**, *32*, 1611; **1999**, *32*, 1714.
(15) Hillebrand, L.; Schmidt, A.; Bolz, A.; Hess, M.; Veeman, W.; Meier, R. J.; van der Velden, G. *Macromolecules* **1998**, *31*, 5010.
(16) Suwelack, D.; Rothwell, W. P.; Waugh, J. S. *J. Chem. Phys.* **1980**, *73*, 2559.
(17) Rothwell, W. P.; Waugh, J. S. *J. Chem. Phys.* **1981**, *74*, 2721.
(18) Takegoshi, K.; Hikichi, K. *J. Chem. Phys.* **1991**, *94*, 3200.
(19) Kuwabara, K.; Horii, F. *Macromolecules* **1999**, *32*, 5600.
(20) Flory, P. J.; Yoon, D. Y.; Dill, K. A. *Macromolecules* **1984**, *17*, 862.
(21) Kitamaru, R.; Horii, F.; Murayama, K. *Macromolecules* **1986**, *19*, 636.
(22) Kimura, T.; Neki, K.; Tamura, N.; Horii, F.; Nakagawa, M.; Odani, H. *Polymer* **1992**, *33*, 4140.
(23) Kitamaru, R.; Horii, F.; Zhu, Q.; Bassett, D. C.; Olley, R. H. *Polymer* **1994**, *35*, 1171.
(24) Parker, J. A.; Bassett, D. C.; Olley, R. H.; Jaaskelainen, P. *Polymer* **1994**, *35*, 4140.
(25) Torchia, D. A. *J. Magn. Reson.* **1978**, *30*, 613.
(26) Kaplan, K. L.; Bovey, F. A.; Cheng, M. N. *Anal. Chem.* **1975**, *47*, 1703.
(27) Saito, S.; Moteki, Y.; Nakagawa, M.; Horii, F.; Kitamaru, R.; *Macromolecules* **1990**, *23*, 3257.
(28) Tsuji, H.; Horii, F.; Nakagawa, M.; Ikada, Y.; Odani, H.; Kitamaru, R. *Macromolecules* **1992**, *25*, 4114.
(29) Möller, M.; Gronski, W.; Cantow, H.-J.; Höcker, H. *J. Am. Chem. Soc.* **1984**, *106*, 5093.
(30) Kuwabara, K.; Kaji, H.; Horii, F. *Polym. Prep. Jpn.* **1997**, *46*, 3565.
(31) Albrecht, T.; Strobl, G. *Macromolecules* **1995**, *28*, 5827.
(32) Opella, S. J.; Waugh, J. S. *J. Chem. Phys.* **1977**, *66*, 4919.
(33) VanderHart, D. L. *Macromolecules* **1979**, *12*, 1232.
(34) Nakai, T.; Ashida, J.; Terao, T. *J. Chem. Phys.* **1988**, *88*, 6049.
(35) VanderHart, D. L. *J. Chem. Phys.* **1976**, *64*, 830.
(36) Reneker, D. H.; Mazur, J. *Polymer* **1988**, *29*, 3.
(37) Noid, D. W.; Sumpter, B. G.; Wunderlich, B. *Macromolecules* **1991**, *24*, 4148.
(38) Sumpter, B. G.; Noid, D. W.; Wunderlich, B. *Macromolecules* **1992**, *25*, 7247.
(39) Zhang, F. *Chem. Phys. Lett.* **1998**, *293*, 499.
(40) Bazeia, D.; Ventura, E. *Chem. Phys. Lett.* **1999**, *303*, 341.
(41) Goldman, M.; Shen. L. *Phys. Rev.* **1966**, *144*, 321.

(42) The segmental exchange with the crystalline component was allowed for the noncrystalline component set parallel to the $+z$ axis in the pulse sequence shown in Figure 8, while the alternative setting parallel to the $+z$ and $-z$ axes was done in the 2D exchange measurement as described in the Appendix. However, since the extent of the T_{1C} correction for the cross-peak intensity was found to be almost the same level for both cases, the average value of 0.1 for the latter case was used here.

MA9912608